ZERO-GRAVITY EFFECTS ON VAPOR COMPRESSION CYCLE PERFORMANCE FOR COLD FOOD STORAGE WITH OIL-FREE SCROLL COMPRESSION

Anthony Skipworth[1], Stephen L. Caskey[1], Leon Brendel[3], Alberto Gomes[2], Rahul Chhajed[2], Sanket Phalak[2], Sanjesh Pathak[2], Eckhard A. Groll[3]

[1] Air Squared, Inc., Broomfield, Colorado,
[2]Whirlpool Corporation, Benton Harbor, Michigan,
[3]Purdue University, West Lafayette, Indiana

ABSTRACT:
NASA and private space organizations have an increasing interest to colonize the Moon and Mars. To establish a thriving human colony on a habitable celestial body, robust and efficient life support systems need to be developed. Currently, astronauts only have access to shelf stable foods in space which do not maintain high nutritional value beyond one-to-three years. A zero-gravity proven cold storage system is necessary to maintain nutritional food for longer durations. A modular refrigerator utilizing a vapor compression cycle (VCC) cooling module was built using a liquid-flooding resilient, oil-free scroll compressor for high robustness and reliability during multi-year missions in zero-gravity. The oil-free operation of the compressor allowed the VCC to operate in zero-gravity due to the mitigation of gravity-dependent oil management systems leveraged in typical refrigeration compressors. The VCC was designed to cool a cabinet to -22 C within the space constraints of two Middeck Lockers (MDL) in a single EXPRESS rack on the International Space Station (ISS). The fabricated refrigeration unit was tested on four parabolic flights with 30, 20-second zero-gravity durations each flight day to characterize the VCC in a simulated space environment. Results from the first and third flight day are presented to discuss the impact on the steady-state operation and pull-down of the cabinet temperature, respectively. The operation of the VCC was stable and suggested that the cycle could provide cooling also in prolonged microgravity. Overall, cabinet temperatures of -20°C were achieved. The evaporator capacity increased during zero-gravity parabolas and returned to its previous value in hyper gravity.

NOMENCLATURE

CAD – Computer Aided Design
EPS – Expanded Polystyrene
EXPRESS – Expedite the Processing of Experiments to the Space Station
ISS – International Space Station
MDL – Middeck Locker
NASA – National Aeronautics and Space Administration
P&ID – Piping and Instrumentation Diagram
RPM – Revolutions Per Minute
SLHX – Suction Line Heat Exchanger
TRL – Technology readiness level
VCC – Vapor Compression Cycle

INTRODUCTION

Utilizing a vapor compression cycle, VCC, refrigeration system for cold food storage in space could play an integral part in meeting the increasing demand of establishing a flourishing human colony on the Moon or Mars. The technology was proposed decades ago (Ginwala, 1961; Hye, 1983; Williams et al., 1973) but has not reached a technology readiness level (TRL) thus far (Leon P.M. Brendel et al., 2021). Currently, astronauts onboard the ISS only eat food that is stored at room temperature which lose their nutritional content over time (Cooper et al., 2017; Smith et al., 2009). To mitigate the concern of food losing nutritional value for astronauts, consumed over a long duration space flight, a VCC refrigeration system was designed and built to store food at -22°C in a zero-gravity environment.

Other refrigeration technologies currently used or used in the past on spacecrafts include thermoelectric cooling, reversed Brayton cycles, and Stirling coolers. Those refrigeration technologies have high TRLs but are less efficient compared to a VCC for temperatures in the typical refrigerator/freezer range. The lower energy efficiency leads to an equivalent mass penalty due to a higher power consumption for the same cooling capacity as pointed out by Brendel et al. (2021).

During the 1980s and 1990s, significant efforts were undertaken to establish vapor compression cycles in zero-gravity. The most frequently flown units were OR/F, EOR/F and LSLE (NASA, 2018a, 2018b also compare with Brendel et al. (2021)). Also Lipson (1982) and NASA (2019) discuss VCCs in space environments. However, none of the previous VCCs in space showed a reliable and good performance and currently only one vapor compression cycle is operational in space (Perry, 2003; Wieland, 1998).

In this paper, a VCC refrigeration system was built and tested on an aircraft performing parabolic flight maneuvers to create a zero-gravity environment for periods of 20-25 seconds. Testing the VCC in a zero-gravity environment will verify that the refrigeration system can reach freezer temperatures and operate without complications in zero-gravity. Some complications that are suspected to arise for a VCC in zero-gravity are as listed in Brendel et al. (2019):

- Liquid entering the compressor suction port during operation
- Liquid slugging from the evaporator during cycle start-up
- Altered heat transfer coefficients in the two-phase flow sections in zero-gravity as compared to ground-based operation
- Oil-management (only for oil-lubricated compressors)
- Condensate management on evaporator coil.

A test stand was designed and built to collect data from the refrigeration system during the parabolic flights. Four zero-gravity flights were utilized over a period of four days to collect data from the refrigeration system. Each flight day had unique testing goals to show that the refrigeration system can achieve freezer temperatures in zero-gravity.

APPROACH

NASA outlined design requirements for an efficient, vehicle-level, cold atmosphere food storage system. The refrigeration system is required to provide a temperature within the range of -80C to 20C inside of the cabinet. A design temperature of -20C was selected based on achieving an efficient, VCC refrigerator with the working fluid selected, R-134a.

The refrigeration system consists of two major parts, the cooling module and the cabinet. The cooling module contains all the VCC components and extracts heat from the cabinet to maintain cold temperatures. The cabinet is the intended location for the cold storage of food. The main components of the cooling module are an oil-free scroll compressor, co-axial tube-in-tube condenser, fin-and-tube evaporator, and a capillary tube for the expansion device. The capillary tube is in contact with the suction line acting as a suction line heat exchanger (SLHX). An oil-free scroll compressor enables the VCC to operate in a zero-gravity environment where oil normally would require gravity driven pooling to maintain lubrication of wearing components. The refrigeration system was designed to fit into two MDLs in a single EXPRESS rack to provide assurances that flight data collected would justify flying the same system configuration on the ISS would work well. Two MDLs have an internal volume of 4 cubic feet which is the amount of space that the cooling module and cabinet must fit within.

Four, zero-gravity flights over the span of four days were utilized with unique testing goals to better understand how the VCC driven, refrigeration system operates in zero-gravity. The focus here is on the results of flight days 1 and 3. The testing goals of each flight day are listed below in chronological order.

1. Understand the effects that zero-gravity has on steady-state operation of the refrigeration system.
2. Determine if liquid enters the compressor suction port during compressor startup when the compressor is cycled on and off in zero-gravity. Investigate which liquid protection methods operate successfully in zero-gravity.
3. Verify that the cooling module can pull down the cabinet temperature to freezer temperatures in zero-gravity and revisit compressor startup at higher speeds.
4. Simulate an overcharged VCC system by power cycling the evaporator fan to remove the heat input to the evaporator. Additionally, operate the compressor continuously at high speeds in zero-gravity.

Flight days 1 and 3 were chosen since the data collected during these tests give an overview of how the VCC refrigeration system is affected by zero-gravity. Flight day 2 and 4 evaluated different aspects of the refrigeration system and will be discussed in a future publication.

<u>Refrigeration System Design:</u>

A modular refrigerator design was selected having a separate cooling module with the refrigerant charged VCC is connected to an insulated cabinet for a cold storage volume. A modular based refrigeration system is beneficial because it allows the volume of the cabinet to be flexible in size.

In case of a larger demand for storage volume, only the cabinet would need to be replaced instead of both the cabinet and cooling module. The approach was applied to sizing constraints for conducting potential future experiments on the ISS. The cooling module design leveraged off-the-shelf components as much as possible to accelerate the development of the refrigerator and enable more time for ground-based testing before the parabolic flights.

Another key decision for the cooling system is related to the type of heat exchanger for the condenser. Since the ISS has an available liquid coolant supply and the compressor will also require cooling, it was decided to use a water-to-refrigerant condenser. In this way the cooling module size can be reduced (minimize weight) and improve the cooling efficiency (minimize power consumption). If the cooling module were to use an air-cooled condenser, the size of the heat exchanger would increase due to the need of extended surfaces (increased surface area) to achieve the desired heat removal rate. Adequate air flow would also need to be supplied to these components which could include the addition of fans adding mass to the system and increasing power consumption. Additionally, liquid cooling over air cooling provides closer approach temperatures which reduces the condensing temperature. Thus lowering the condensing pressure and ultimately decreasing compressor work with reduced pressure differentials or ratios.

Figure 1 shows a CAD model of the cooling module and cabinet separated from each other. The cooling module itself is divided into a hot and cold section based on the operating temperatures of the major components. The hot side contains the compressor and condenser while the cold side contains the evaporator. The evaporator is encased in EPS foam to reduce the external heat gain from other sources outside of the cabinet cavity. Note that the cooling module extends further than the cabinet in Figure 1. The cooling module is slightly oversized due to the need of instrumentation to collect data and to reduce complexity addressing issues that could arise on the zero-gravity flights. The use of off-the-shelf components also contributed to the cooling module being tight on space since the dimensions of the VCC components could not be altered. If components were custom made, the size of the cooling module could be packaged to fit within the space constrains of 2 MDLs. A benefit of adding clearances in the cooling module is that it is easier to service and maintain.

Figure 2 shows a piping and instrumentation diagram (P&ID) of the VCC cooling module. Each component is defined in the legend and the fluid states are identified with different colors and line styles. Note that there are no mass flow measurements, air speed measurements, or air humidity measurements referenced in the P&ID since these sensors could not fit within the space constraints of the refrigeration system. Starting at the compressor, low pressure, superheated R-134a vapor is drawn in and discharges high pressure, superheated vapor which is fed into the condenser. The superheated R-134a vapor is condensed to a subcooled liquid in a standard VCC operation and can potentially exit as a two-phase mixture, vapor and liquid, with a passive expansion device such as a capillary tube. The condensed R-134a passes through a sight glass referred to as the liquid sight glass to visually confirm the refrigerant state supplied by the

condenser. For this VCC system, a full liquid sight-glass was not observed which would normally negatively impact a traditional expansion device. However, the capillary tube did not show signs of choked flow with a two-phase inlet state and was forgiving to this type of VCC operation.

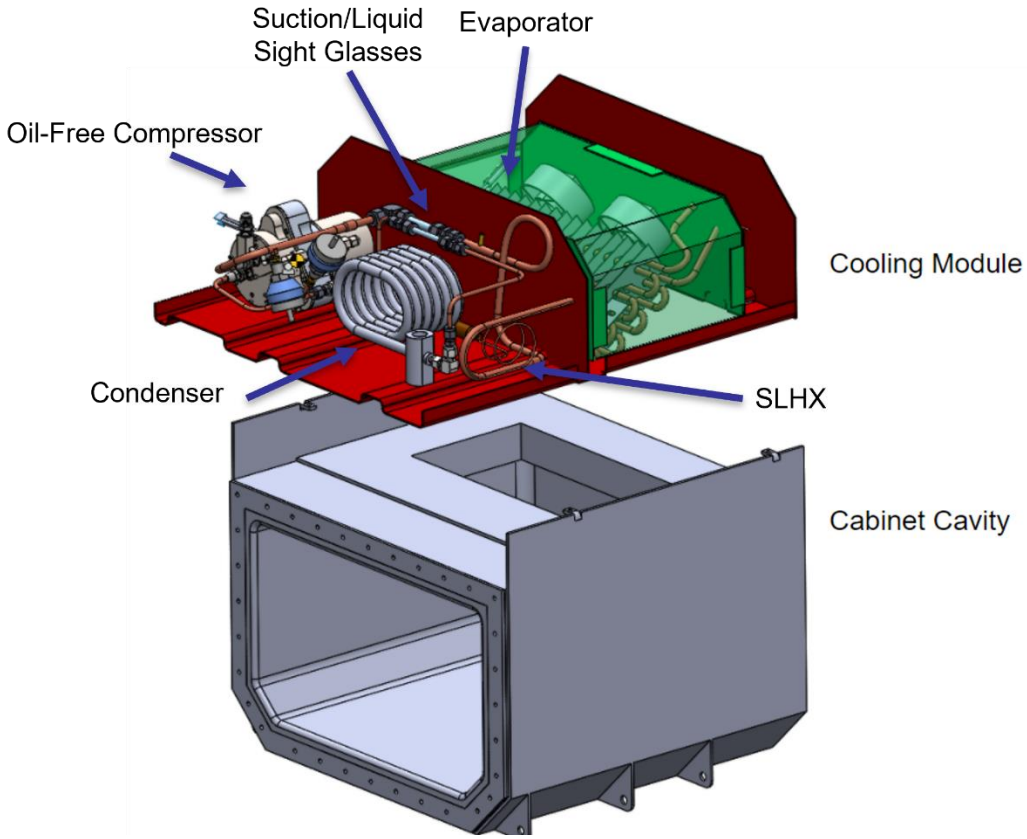

Figure 1: CAD Model of Refrigeration System Final Design

The subcooled R-134a continues through the liquid sight glass to the filter/drier to remove any debris or moisture in the refrigerant. With a proper charging approach, the presence of moisture in the system should be controlled. The use of small area devices for expansion (pressure drop) could be blocked if any debris in the system reaches this component. In the capillary tube, the high-pressure, R-134a liquid expands into a low-pressure, two-phase mixture due to frictional pressure drop long the length of the capillary tube. Upon entering the evaporator, heat is extracted from the cabinet by boiling off the liquid in the two-phase flow. Low pressure, superheated vapor exits the evaporator and picks up heat from the capillary tube which is expanding high pressure liquid that comes out of the condenser. The capillary tube acts as a suction line heat exchanger and is a compressor suction liquid protection method. The SLHX boils off any remaining liquid leaving the evaporator in the suction line giving increased confidence that liquid refrigerant will not enter the compressor suction port. Transferring heat from the high-pressure liquid exiting the condenser results in a hotter, and reduced density inlet state to the compressor decreasing its isentropic efficiency. Although the compressor's isentropic efficiency is negatively impacted, the enthalpy of R-134a at the evaporator inlet is reduced by increasing

the amount of liquid to vapor refrigerant, allowing more heat to be extracted from the cabinet theoretically increasing the cooling capacity. Liquid cooling was supplied to the condenser and compressor via a pressurized water loop. The loop was recharged by using an air-cooled radiator to reject heat directly into the airplane cabin. The impact of the changing airplane environmental air temperature during the flights resulted in different water supply temperatures to the refrigeration system.

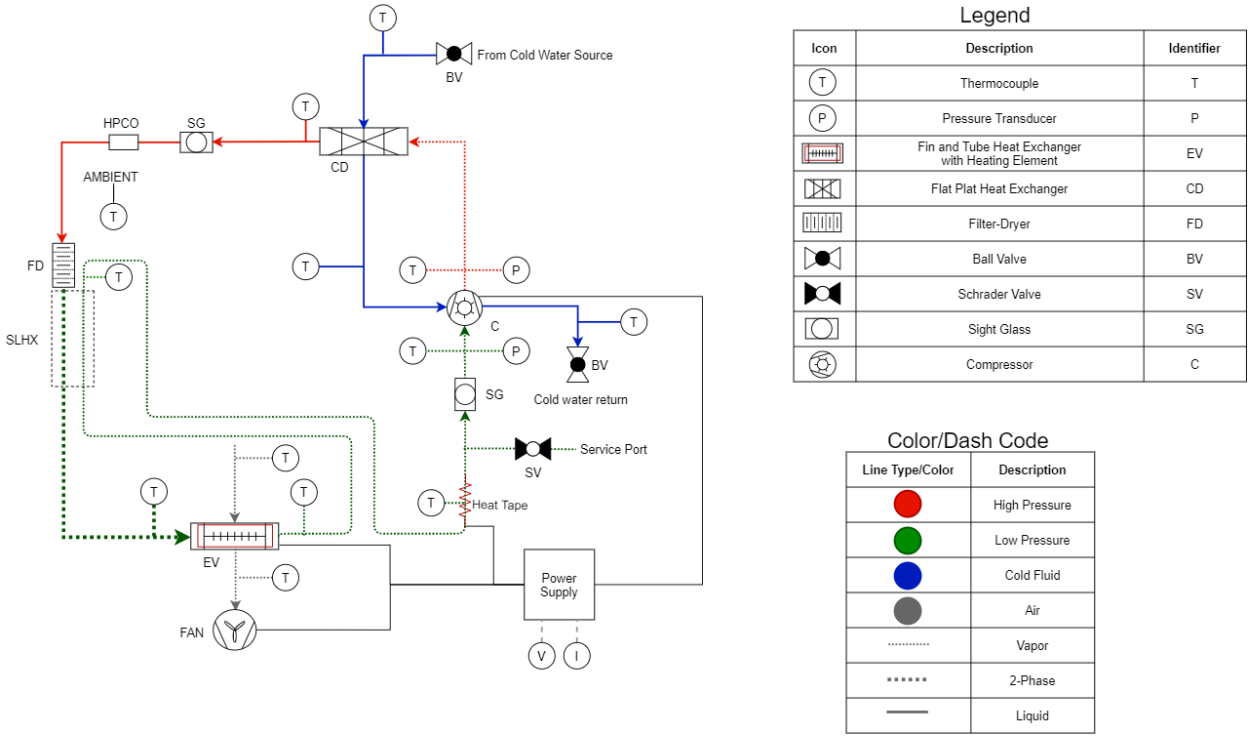

Figure 2: Vapor Compression Cycle Cooling Module Piping and Instrumentation Diagram

DATA COLLECTION

Measurements and data processing:

Raw data was processed using MATLAB with REFPROP calls to compute fluid properties of R-134a. Refrigerant temperatures were measured at the inlet and outlet of each component in the VCC with surface thermocouples. Air temperatures were measured at the in and outlet of the evaporator. Refrigerant pressure is only measured at the compressor suction and discharge. Periods of zero-gravity were measured using an accelerometer. The performance of the compressor is quantified by the volumetric efficiency and isentropic efficiency but requires a refrigerant mass flow rate. Without a direct measurement, ground testing was used to apply conservative volumetric efficiencies to estimate the refrigerant flow rate during the flights. The rate of heat removal from the cabinet is calculated from the refrigerant side evaporator capacity with the estimated refrigerant flow rate.

ZERO-GRAVITY TEST RESULTS

Flight Day 1 – Steady-State Operation:

The testing goal during the first flight day was to capture the transient effects of fluctuating gravity levels on the steady-state operation of the VCC. The aircraft performed 5 consecutive zero-gravity maneuvers which was defined as a set of parabolas and followed by a level flight break which lasted for about 3-5 minutes. In Figure 3, the acceleration of the aircraft is plotted with the cabinet temperatures and evaporator temperature. The first set of zero-gravity parabolas started around a test time stamp of 10:30 and the last set of parabolas occurred around a test time stamp of 11:30. The compressor speed was increased by 200RPM after 2 sets of zero-gravity parabolas to investigate if the effect that zero-gravity has on the VCC is diminished or amplified with a new compressor speed. The compressor ran at a speed of 2400 RPM for parabola sets 1-2, 2600 RPM for parabolas sets 3-4, and 2800 RPM for parabola sets 5-6.

To ensure that the system was at steady-state before the first zero-gravity parabolas, the compressor and cooling loop were turned on while the aircraft was on the ground to pull down the cabinet temperature. Ground testing showed that approximately 1.5 hours of compressor operation were needed for the cabinet to reach a steady-state temperature. Figure 3 shows the cabinet temperatures and evaporator temperatures during the zero-gravity flight. The cabinet return temperature, identified by the red line, represents the air temperature being drawing into the evaporator and is most representative of cabinet air temperature. The supply temperature, identified by the blue line, represents the air temperature exiting the evaporator. The cabinet reaches a steady-state temperature of -14C at a test time stamp of 10:05 before the zero-gravity maneuvers begin. Figure 3 shows that the evaporation temperature varies by several degrees of Celsius due to the gravity fluctuations but that those changes are too short to propagate strongly into the air temperatures. Instead, the air return temperatures are mildly affected, and the supply temperatures are stable.

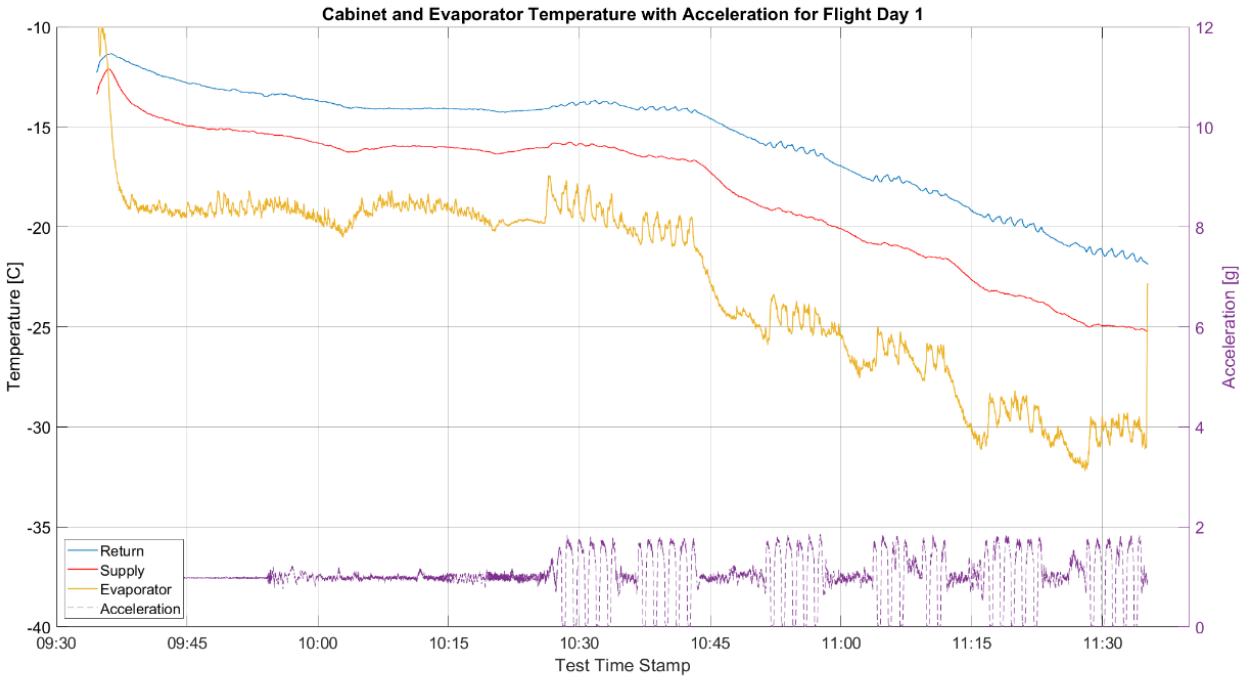

Figure 3: Cabinet and Evaporation Temperature with Acceleration for Flight Day 1

The fluctuations in cabinet return temperature in zero-gravity can be better visualized by focusing on one parabola set in flight day 1. Figure 4 shows the cabinet return and supply temperature with the acceleration of the aircraft for the 5th parabolas set. The 5th parabola set was chosen because the magnitude of cabinet temperature fluctuations was greatest during the 5th and 6th parabola set during flight day 1. As could be seen in Figure 4, the supply temperature is not affected by the flight maneuvers. The reason is that the cabinet itself acts as large enough buffer to level out the small variations of the return temperature.

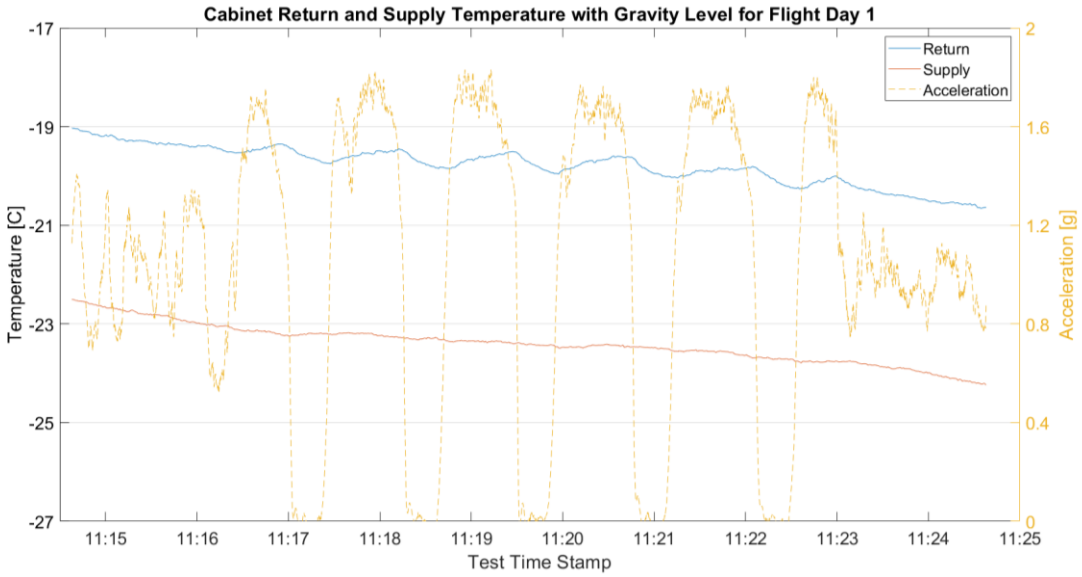

Figure 4: Cabinet Return and Supply Temperature with Gravity Level for 5th Parabola Set in Flight Day 1

Figure 5 shows the operational compressor speed during the flight with refrigerant suction and discharge pressures. Increasing the compressor speed can be noticed in the suction pressure decreasing due to the capillary tube being a passive expansion device. The small fluctuations in the suction pressure indicate a period of zero-gravity and are neither detrimental to the cycle performance nor to the compressor operation. Note that the compressor discharge pressure decreases through the entire flight. The direct impact of the decreasing water temperature in the cooling loop results in the compressor operation not being a true steady state operation.

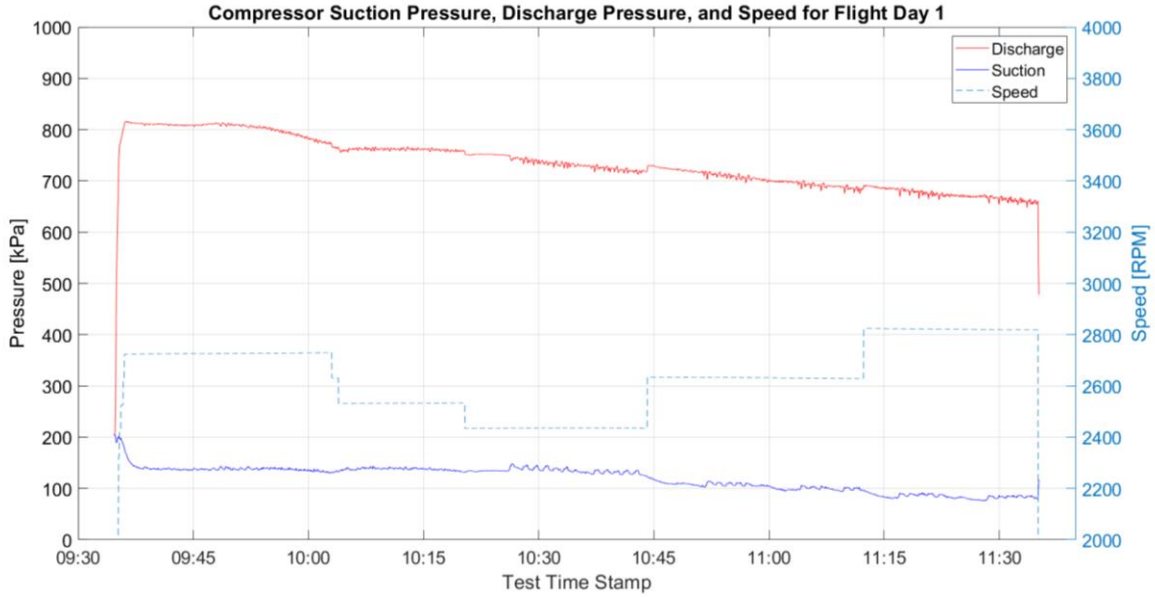

Figure 5: Compressor Pressure and Speed for Flight Day 1

Due to the absence of mass flow measurement on the refrigeration system, previous volumetric efficiencies of 50% - 70% from ground testing had to be utilized for calculating a mass flow rate. A compressor volumetric efficiency of 50% was used as a conservative estimate to assume the mass flow rate through the refrigeration circuit during the flights using a calculated ideal mass flow rate. The ideal mass flow rate is calculated from the known compressor suction volume of 4.53cc, compressor speed and suction density, the latter being calculated from the measured refrigerant inlet temperature and pressure. The calculated mass flow rate and refrigerant side evaporator inlet and outlet enthalpy is used to calculate the refrigerant side cooling capacity of the evaporator. The outlet enthalpy is calculated from the outlet vapor of the evaporator with temperature and pressure while the inlet enthalpy required an energy balance on the SLHX to estimate an evaporator inlet enthalpy. Figure 6 shows the refrigerant side evaporator capacity with a compressor volumetric efficiency of 50% and the gravity level during the 5th set of zero-gravity parabolas. The evaporator capacity increases from 70 W before the parabola set starts and increases to 80 W during periods of zero-gravity resulting in a 14% increase in cooling capacity. The cooling capacity does not decrease to 70 W during hyper gravity but only after the set of parabolas is completed. For the first, third and fifth parabola, the cooling capacity increases already before the gravity measurement falls below $1g$. It is therefore possible that effects of hyper gravity contribute to the increased cooling capacity observed during zero-gravity. Given the inherently slow time constants of surface thermocouple measurements and heat exchanger balances used in the computation of the cooling capacity, a longer microgravity time window would be required to gain confidence.

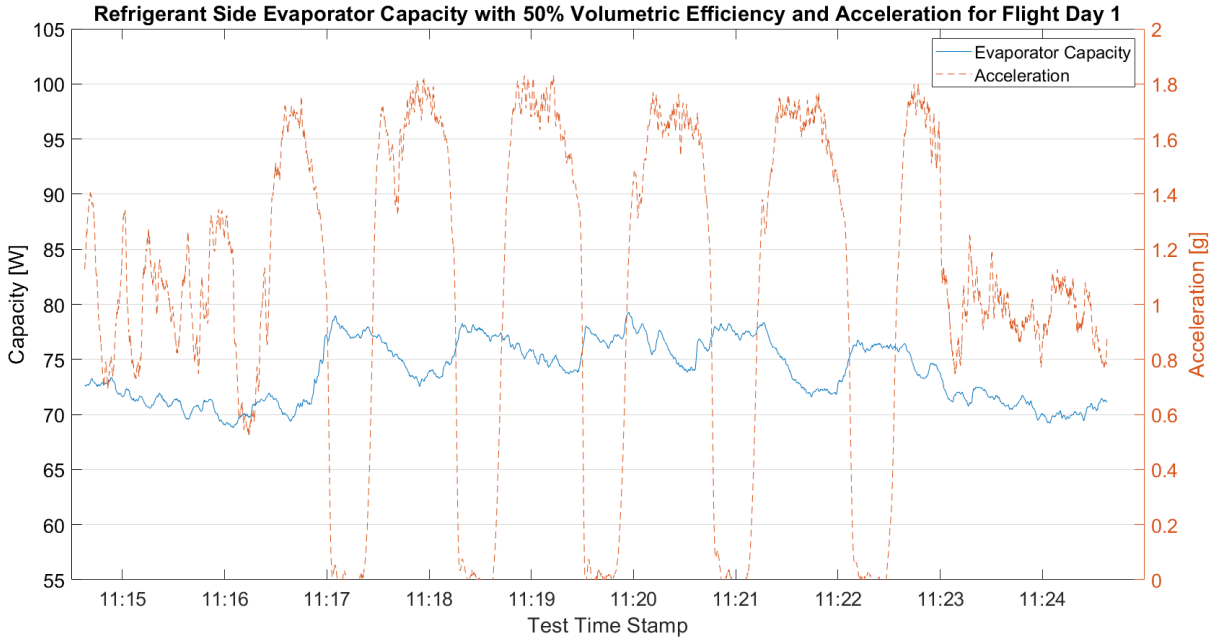

Figure 6: Refrigerant Side Evaporator Capacity with assumed 50% Volumetric Efficiency and Measured Gravity Level for Flight Day 1

Flight Day 3 – Pulldown and Compressor Cycling:

The testing goal during the 3rd zero-gravity flight day was to pull down the cabinet temperature to freezer temperatures starting at ambient conditions through varying gravity levels. Once the cabinet is at a steady-state temperature, compressor start-up at higher speeds were recollected to obtain additional data. The system was left off during take-off. Approximately 1 minute before the zero-gravity maneuvers began, the compressor was ramped up to 2400 RPM, the cooling loop was activated, and the evaporator fan was turned on. For the first set of zero-gravity parabolas, the compressor speed was maintained at 2400 RPM. After the first set of parabolas, the compressor speed was increased to 2600 RPM to pull down the cabinets faster. After the third set of parabolas, the compressor was turned off since the cabinet reached freezer temperature and the testing focus shifted to compressor cycling. For the 4th and 5th set of parabolas, the compressor was cycled on during periods of zero-gravity and off right before the zero-gravity period ended to investigate if liquid would enter the compressor suction port. For the 5th set of parabolas, the compressor was turned on at a higher speed of 3000 RPM to investigate if a higher speed would eliminate suction line liquid flooding. The results from cycling the compressor are discussed in a future, separate publication. For the last set of parabolas, the compressor was left to run continuously at 3000 RPM to pull down the cabinets as much as possible for the remainder of the flight and investigate if higher speed operation provided different results than previously evaluated speeds.

Figure 7 shows the compressor inlet pressure, outlet pressure, and compressor speed for the duration of flight day 3. Before the first set of zero-gravity parabolas, there is no pressure differential across the compressor as both inlet and outlet pressures are at their respective resting pressure. When the compressor is first turned on, the discharge pressure spikes and then begins to follow the same trend observed in flight day 1. The compressor starts off at a speed of 2400 RPM for the first set of parabolas and then is increased to 2600 RPM to pull down the cabinet temperatures more aggressively. Given the short time frame of 3 parabola sets for a pull down, a speed of 2400 RPM would not be able to pull the cabinet temperature down to freezer temperatures. A slight increase in speed to 2600 RPM was selected to ensure that the cabinet temperatures would reach freezer temperatures in the given parabolic flight time window.

A plot of the cabinet temperatures, evaporator temperature, and ambient temperature is shown in Figure 8. The cabinet return and supply temperature decrease the fastest at the beginning of the pull down due to a large temperature differential between the cabinet air temperature and the evaporation temperature. After the 3rd set of zero-gravity parabolas, around a test time stamp of 10:40, the cabinet return and supply temperature start to decrease at a slower rate and approach a steady-state temperature. As seen in flight day 1, the evaporation temperature fluctuates during parabolas which mildly affects the return temperature but not the supply temperature. The hypothesis based on the data is that the cabinet temperature would decrease at a faster rate onboard a spacecraft than on the ground. However, this could only be verified with an orbital testing opportunity.

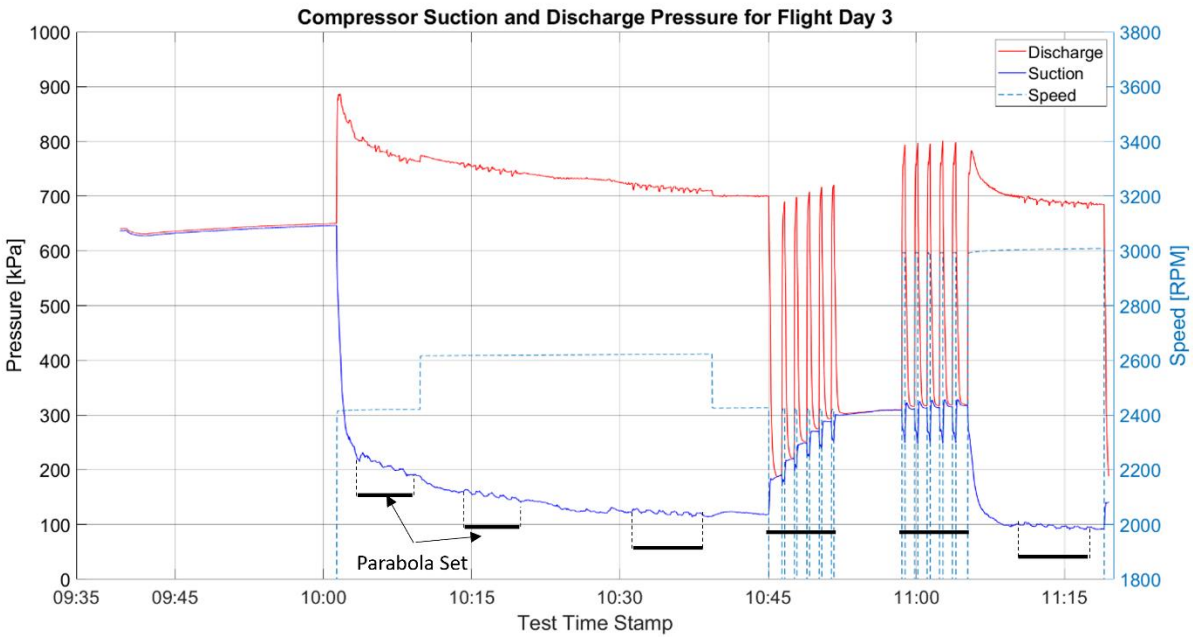

Figure 7: Compressor Pressures and Speed for Flight Day 3

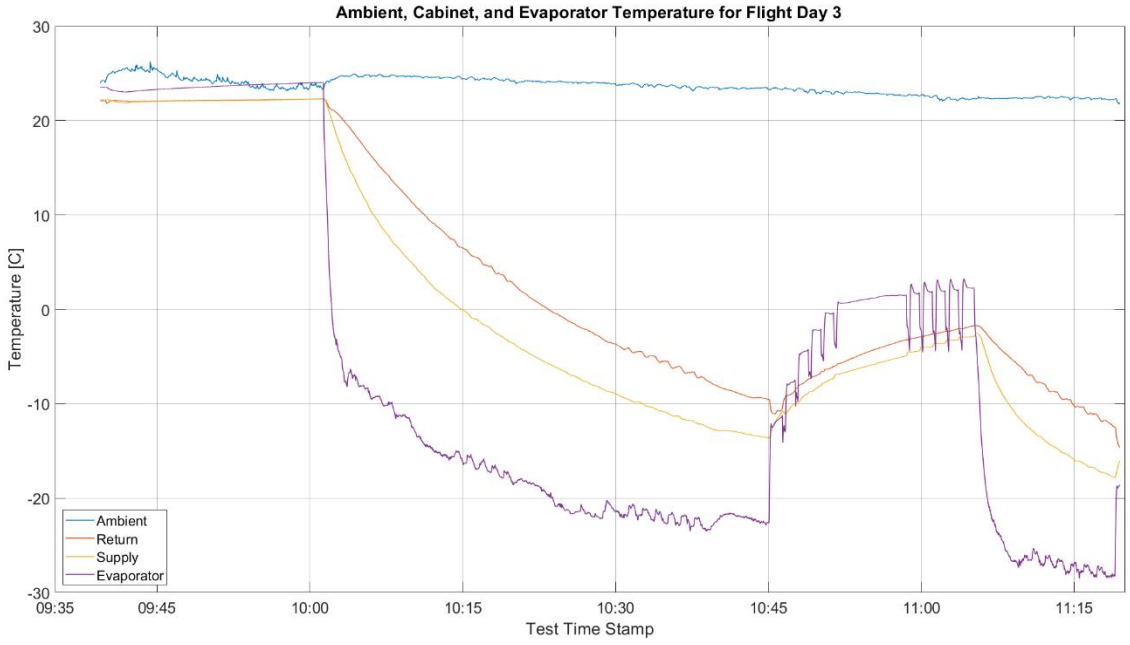

Figure 8: Cabinet, Evaporator, and Ambient Temperatures for Flight Day 3

During the last set of parabolas, time stamp 11:10, the compressor operated at a speed of 3000 RPM. A higher compressor speed results in higher mass flow rates. With a passive expansion valve, the expanded refrigerant flow rate is lower than the increase in flow from the compressor. As a net effect, the suction pressure decreases which results in a lower evaporation temperature.

A larger temperature difference between the evaporator and cabinet results in a higher rate of heat removed from the cabinet at this higher compressor speed.

DISCUSSION

Flight Day 1 – Steady-State Operation:

The most significant observations in flight day 1 are the fluctuations in cabinet temperature, fluctuations in evaporation temperature, and increase in evaporator capacity during periods of zero-gravity. Referring to Figure 4, one hypothesis explaining the decrease in cabinet return temperature and constant supply temperature is the increase in heat removal from the evaporator coils due to the annular flow regime in zero-gravity inside the evaporator tube walls. During every zero-gravity period, the two-phase flow regime transitioned from stratified flow to annular flow as observed in the liquid sight glass. The annular flow regime means that the entire surface of the evaporator pipe wall is coated in liquid compared to stratified flow where about 40% of the pipe wall is coated with liquid. Since the entire pipe wall is coated in liquid, more pipe surface area is available to boil refrigerant, increasing the rate of heat transfer from the cabinet. The increase in heat transfer rate is expected to overcome the decreased temperature difference between the evaporator temperature and supply temperature resulting in a net decrease in cabinet supply temperature.

Another hypothesis as to why the cabinet return temperature decreases during periods of zero-gravity is that the fan velocity changes in zero-gravity. Without the force of gravity pushing on the fan, there is less friction on the fan bearings allowing it to rotate faster given the same power input. An increase in fan rotational speed increases the air velocity over the evaporator coils resulting in the air side evaporator capacity increasing. This increase in air side evaporator capacity allows more heat to be removed from the cabinet causing the cabinet return temperature to decrease. The uncertainty in this hypothesis is because there was no direct air velocity measurement inside the cabinet during all of the flight days to confirm a higher airflow rate measured during zero-gravity parabolas.

In Figure 6, the calculated evaporator capacity increases during every zero-gravity period. Most likely this is due to the increase in suction pressure during periods of zero-gravity. The ideal mass flow rate depends on the refrigerant suction density of the compressor. A rise in suction pressure corresponds to an increase in suction density. The greater the suction density, the higher the ideal mass flow rate which propagates out to a higher refrigerant side evaporator capacity. The elevated refrigerant side capacity in zero-gravity supports the hypothesis of the decrease in cabinet return temperature during periods of zero-gravity.

An increase in evaporator capacity is thought to correspond to a decrease in both the cabinet return and supply temperature while an increase in evaporator temperature is expected to create the opposite result. As stated earlier in this section, this is not the case since the cabinet return temperature decreases while the cabinet supply temperature remains constant during periods of zero-gravity. Since the evaporator temperature is elevated during periods of zero-

gravity but the evaporator capacity increases, this potentially creates a net zero change in the cabinet supply temperature. This would draw conclusions toward the cabinet return temperature being influenced only by the evaporator capacity while the cabinet supply temperature is influenced by both the evaporator capacity and temperature.

Flight Day 3 – Pulldown and Compressor Cycling:

The results from flight day 3 have similar trends to the results in flight day 1. One major difference is the VCC started at ambient conditions in flight day 3 while the VCC was already at steady state before the first set of parabolas in flight day 1. When the compressor is initially turned on, the cabinet temperatures decrease at the fastest rate. At this point, the temperature difference between the evaporator and cabinet supply is greatest. The air side evaporator capacity is assumed to be largest when the temperature difference between the evaporator and the supply temperature is at a maximum. Humidity and air speed measurements across the evaporator are necessary to calculate the air side evaporator capacity. Since these measurements were not available due to space constraints of the system, the air side evaporator capacity is unidentified. A plot of the temperature difference between the evaporator and cabinet supply as well as the temperature difference between the cabinet return and cabinet supply can be referred to in Figure 9.

The temperature difference between the cabinet supply and return temperature decreases from 20C to 10C while the temperature difference between the evaporator and cabinet experiences a 1C decline over the first 3 sets of parabolas. A possible reason the temperature difference between the cabinet return and supply decreases over time is due to frost formation on the evaporator coils acting as heat exchanger fouling. Although it may seem intuitive, the temperature difference between the cabinet return and supply is not a good indicator of evaporator fouling and heat exchanger effectiveness. As the cabinet temperatures continue to pull-down, the cabinet temperature approaches the evaporator temperature which could cause a reduction in the evaporator temperature difference on the air side.

Since the cooling capacity usually increased during the microgravity section of one parabola, it is hypothesized that a VCC refrigeration system in space could operate for shorter duty cycles since the cabinet will reach the cabinet temperature setpoint sooner. Shorter duty cycles could increase the lifespan of the refrigeration system and the higher cooling capacity would increase the flexibility of the cabinet size by coupling to larger volumes. One consequence of an increased capacity is the expansion of cycling losses; however, the refrigeration system would be optimized to minimize these losses by leveraging smaller compressor suction volumes or operating at lower speeds.

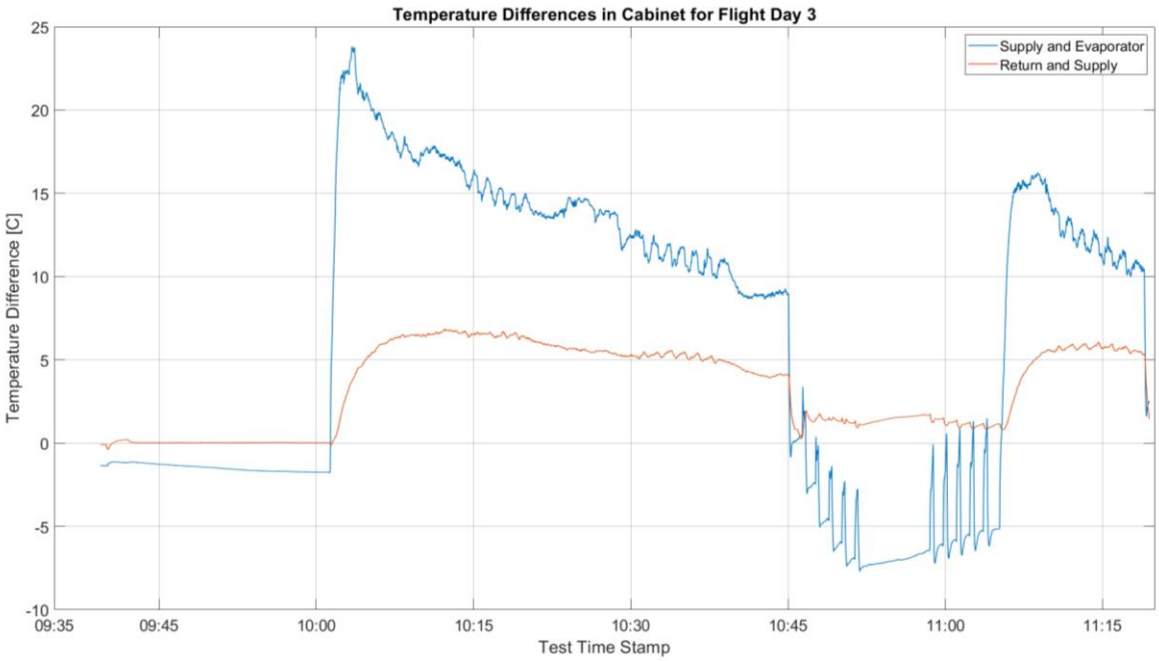

Figure 9: Temperature Differences in Cabinet for Flight Day 3

CONCLUSIONS

A vapor compression cycle with an oil-free compressor was prototyped and tested on four parabolic flights with 30 parabolas each. Flight day 1 alluded to an increased cooling capacity in zero-gravity periods compared to the preceding and succeeding hyper gravity. This was explained by an increased evaporation temperature and pressure leading to increased refrigerant mass flow rates. The gain in evaporator capacity in zero-gravity is reflected by a decrease in cabinet return temperatures. Flight day 3 verified that a cabinet temperature pull-down to freezer temperatures through alternating zero and hyper gravity levels was possible, too. Since the duration of the zero-gravity parabolas are short, steady-state operation of the VCC in zero-gravity has yet to be characterized. Additional testing in a sustained zero-gravity environment is motivated by promising results during alternating gravity levels to fully understand how the VCC operates in zero-gravity.

ACKNOWLEDGEMENT

The authors greatly appreciate the support of this work by NASA under SBIR contract 80NSSC18C0049 is gratefully acknowledged with Michael Ewert's guidance and Alexander Van Dijk's support. This experiment would not have been possible without major support from Robert Greeno and Robert Brophy in Air Squared's technical shop. Thanks to Alain Bucio from Air Squared for documenting the zero-gravity flight experience. The financial and technical support from Whirlpool is very much appreciated.

REFERENCES

Brendel, L.P.M., Braun, J.E., Groll, E.A., 2019. Matching Testing Possibilities and Needed Experiments for Successful Vapor Compression Cycles in Microgravity. Presented at the 3rd International Conference for Refrigeration and Cryogenic Engineering, Air Conditioning and Life Support Systems, Moscow, Russia.

Brendel, Leon P M, Caskey, S.L., Ewert, M.K., Gomes, A.R., Braun, J.E., Groll, E.A., 2021. Equivalent Mass Benefits from Employing Vapor Compression Refrigeration on Spacecraft. Presented at the International Conference on Environmental Systems 2021, Lisbon, Portugal (Virtual Conference), p. 12.

Brendel, Leon P.M., Caskey, S.L., Ewert, M.K., Hengeveld, D., Braun, J.E., Groll, E.A., 2021. Review of vapor compression refrigeration in microgravity environments. International Journal of Refrigeration 123, 169–179. https://doi.org/10.1016/j.ijrefrig.2020.10.006

Cooper, M., Perchonok, M., Douglas, G.L., 2017. Initial assessment of the nutritional quality of the space food system over three years of ambient storage. npj Microgravity 3. https://doi.org/10.1038/s41526-017-0022-z

Ginwala, K., 1961. Engineering study of vapor cycle cooling equipment for zero-gravity environment (Technical report No. TR 60-776). Wright-Patterson Air Force Base, Dayton, OH, USA.

Hye, A., 1983. The Design and Development of a Vapor Compression Refrigerator/Freezer for Spacelab. Presented at the 13th Intersociety Conference on Environmental Systems, San Francisco, California.

Lipson, D., 1982. STS-4 Postflight Final Report for the Vapor Phase Compression Refrigerator/Freezer (Technical Information Release No. DTO No. 467).

NASA, 2019. Refrigerated Centrifuge (RC) [WWW Document]. International Space Station. URL https://www.nasa.gov/mission_pages/station/research/experiments/explorer/Investigation.html?#id=629

NASA, 2018a. Orbiter Refrigerator/Freezer Hardware Information Guide [WWW Document]. Life Sciences Data Archive. URL https://lsda.jsc.nasa.gov/Hardware/hardw/64

NASA, 2018b. Life Sciences Laboratory Equipment Refrigerator/Freezer Hardware Information [WWW Document]. Life Sciences Data Archive. URL https://lsda.jsc.nasa.gov/Hardware/hardw/18

Perry, J.L., 2003. Octafluoropropane Concentration Dynamics on Board the International Space Station, in: SAE Technical Paper Series. Presented at the 33rd International Conference on Environmental Systems, Vancouver, B. C., Canada. https://doi.org/10.4271/2003-01-2651

Smith, S.M., Zwart, S.R., Kloeris, V., Heer, M., 2009. Nutritional Biochemistry of Space Flight. Nova Science Publishers.

Wieland, P.O., 1998. Living Together in Space: The Design and Operation of the Life Support Systems on the International Space Station (No. NASA/TM-1998-206956/Volume II). NASA, George C. Marshall Space Flight Center, Huntsville, AL.

Williams, J.L., Keshock, E.G., Wiggins, C.L., 1973. Development of a Direct Condensing Radiator for Use in a Spacecraft Vapor Compression Refrigeration System. Journal of Engineering for Industry 95.